UPGRADE PROGRAMME – PHASE I

UPBL CONCEPTUAL DESIGN REPORT

UPBL10: Massively automated sample selection integrated facility for macromolecular crystallography	
Current designated sector:	Facility goes to:
ID14	ID30 and BM29

1.1 SUMMARY

Structural Biologists are tackling ever more ambitious projects, for example more complex membrane proteins and larger macromolecular assemblies. Such systems often show considerable inter- and intra-crystal variation in diffraction quality. Sample evaluation prior to data collection, already widespread in Macromolecular Crystallography (MX), will thus become more crucial as will data collection facilities optimised for the collection of diffraction data from crystals that are very small and/or diffract to low resolution (i.e. d_{min} 4 to 5 Å).

UPBL10 will be a unique resource, based on 2nd generation automation for MX experiments, designed to maximise the chances of a successful conclusion to these ambitious projects. The hub of the facility is a sample evaluation and sorting facility (MASSIF). The most suitable crystals from which to collect data will be distributed from MASSIF to the data collection facilities that form an integral part of this proposal as well as to refurbished resources on ID29 and ID23.

1.2 PROJECT HISTORY

The most recent review of the ESRF's MX beamlines was undertaken in November 2006 when all operational beamlines were considered as an integrated suite. At the same time as acknowledging the scientific and technological impact of the MX beamlines, the Review Committee recommended that the MX group initiate an appraisal of the beamlines' technologies and, in particular, look into models for upgrading ID14 A&B. Subsequent analysis and consultation with the ESRF's MX User Community resulted in the ideas contained within the Purple Book. A series of consultation meetings with the MX User Community has subsequently taken place. The last of these meetings, the UPBL10 brainstorming, was held in order to distill the input received and, at the specific request of the ESRF SAC meeting held in November 2007, to *produce a coherent, user-driven scientific case for the upgrade of ESRF MX resources.* The resulting case, produced after the meeting, forms a significant part of this document. The second major outcome of these meetings was the definition of a resource that would take advantage of the major infrastructure aspects of the ESRF Upgrade Programme, be unique to the ESRF, and provide a resource that would satisfy the needs of the European Structural Biologists for the next 10 to 20 years.

1.3 SCIENTIFIC CASE

There has been a dramatic growth in MX over the last 15 years. This growth has been coupled with some spectacular scientific successes. These have been achieved across the whole spectrum of biology including (but not limited to) membrane proteins (G-protein coupled receptors (Warne et al, 2008), ABC transporters (Dawson & Locher, 2006), ion channels (cited in the 2003 Nobel prize for chemistry (Doyle et al, 1998)), photosystems I and II (Ben-Shem et al, 2003; Ferreira et al, 2004; Zouni et al, 2001)), viruses (Blue tongue virus (Grimes et al, 1998) and more recently lipid bilayer containing bacteriophages (Cockburn et al, 2004)), molecular machines (F_1-ATPase (cited in the 1997 Nobel prize for chemistry) (Walker, 1998)), the bacterial ribosome (Schlunzen et al, 2001; Selmer et al, 2006, Nobel Prize in 2009), DNA polymerase II (cited in the 2006 Nobel prize for chemistry (Cramer et al, 2001)), the muscle contractile protein myosin (Coureux et al, 2003), macromolecular complexes (the proteosome (Groll et al, 1997), tumour necrosis factor (Liu et al, 2003)), high throughput ligand screening for improved medicines (human cytochrome P450 (Williams et al, 2004; Williams et al, 2003) and human phosphodiesterase structures (Sung et al, 2003)) and the development of new tools for medicine and cell biology (Green Fluorescent Protein (GFP) (cited in the 2008 Nobel prize for chemistry) (Ormo et al, 1996)). The impact of these results has extended from an improvement of the basic understanding of Molecular Biology to wealth generation in the European Community.

Advances in technology have played a significant role in these achievements. For MX this has included improvements in protein expression and crystallisation and, crucially, the development of intense, tuneable beamlines at third generation synchrotron sources. Within the last five years, three further developments at synchrotrons have played important roles, namely high levels of automation of sample handling, automation of X-ray beam delivery and good access to microfocus beamlines that are optimised for MX applications. The ESRF has played a world-leading role in all of these areas (Beteva et al, 2006; Flot, 2008).

Spurred on by the successes that have already been achieved, Structural Biologists are tackling ever more ambitious projects, for example the large assemblies involved in the human complement pathway of innate immunity (Central complement protein C3 – a complex of 13 distinct domains solved by Piet Gros and co-workers (Janssen et al, 2005)). Almost invariably, these projects pose significant challenges both in terms of specimen preparation and in terms of obtaining sufficient material of the appropriate levels of purity and stability for crystallisation trials. This is particularly an issue for mammalian membrane proteins, which are very unstable in the detergents that are used for crystallisation, and for which the cost of obtaining sufficient quantities of sample is extremely high.

In the context of this report, it is particularly relevant to note that it is very common for crystals of biological macromolecules, even when obtained under notionally identical conditions, to show considerable variation in the quality of their diffraction. This is almost certainly due to the intrinsic physical properties of the systems being studied. The molecules involved are often very flexible, leading to conformational heterogeneity. In the case of complexes of several proteins, there is also the risk of compositional heterogeneity where some complexes have lost one or more components. When the crystals obtained are small (<50 μm) they are also often

mechanically fragile, and therefore susceptible to damage during transfer (from the crystallisation trays to the sample holders) or essential cryoprotection steps.

Current data collection trends at the ESRF MX beamlines show clearly that automation has led to a fundamental change in the way that MX data are collected. With the introduction of the automatic sample changer (SC3) at the ESRF MX beamlines in 2005, a dramatic increase in the number of samples that were tested for diffraction quality before any full data collections were carried out was observed (Figure 1). Automation has had a spectacular effect on the scientific output of the ESRF MX beamlines (Table 1). Over the past seven years there has been a more than three-fold increase in the number of structures elucidated using data collected at the ESRF. Although the output has increased - MX beamlines now produce over a quarter of the publications from the ESRF - this has not been at the cost of quality. The scientific impact of the experiments remains extraordinarily high, with around 20% of publications appearing in journals with an impact factor greater than 10. **Automation of synchrotron beamlines thus not only increases scientific output but it also maintains the high-level impact of the science performed**.

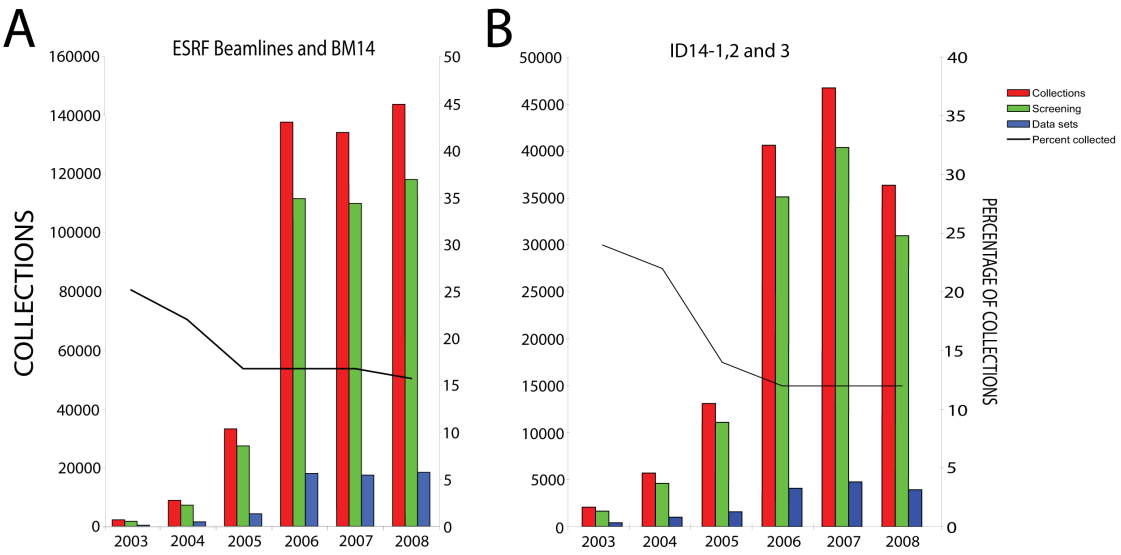

Figure 1. MX sample screening and data collection at the ESRF (data harvested from the ISPyB database). A: ESRF MX beamlines and BM14. The number of total collections, screenings and data sets are shown in the bar chart. The percentage of samples on which data are eventually collected is shown as black line. B: Beamlines ID14-1, 2 and 3 (*14-3 was recommissioned as a bio-SAXS beamline at the end of 2007, therefore, statistics for 2008 are for 14-1 and 2 only).* These beamlines are heavily used for sample evaluation. The percentage of samples from which full data sets are collected has fallen steadily to 11% in 2007 (Screens are defined as ≤4 images and a data set is defined as ≥30 images).

Year	Total ESRF PDB Depositions	Total MX ESRF Publications (From ESRF Library Database)	Publications Impact factor > 10.0	% Publications Impact Factor > 10.0	% of MX publications out of total ESRF publications
2001	215	165	47	28	14
2002	295	239	63	26	20
2003	413	297	63	21	22
2004	484	364	75	21	26
2005	586	328	64	20	22
2006	637	417	91	22	27
2007	681	428	86	20	26

Table 1. Data deposition and publication statistics for ESRF MX beamlines.

Some specific examples illustrate the current situation. G-Protein Coupled Receptors (GPCRs) are the largest family of membrane proteins in the human genome and are involved in the control of many physiological processes. It is estimated that GPCR targeted drugs account for 50% of the current market for human therapeutics (e.g. β-blockers, treatments for asthma, mood control), and there is considerable pharmaceutical interest in their three-dimensional structures. The structure of the GPCR β_1-adrenergic receptor was recently determined using data collected at the microfocus beamlines at the ESRF (the crystals are typically <20 μm thick). However, 1043 crystals were screened over a period of ten months before a well diffracting crystal was obtained (Warne et al, 2008), bringing to a conclusion more than 18 years of effort on this project. Access to a facility that provided a microfocused beam was vital to prove the viability of the project. **However, success could only be achieved via the combination of a microfocused beam and a highly automated beamline control.**

A second example is the structure of the bacterial 70S ribosome, the complex responsible for the RNA directed synthesis of bacterial proteins. Understanding the structure of the ribosome and the complexes it forms with various additional components provides fundamental information on the cellular generation of proteins. The ribosome is also the target for many antibiotics. The 70S ribosome is composed of 53 protein molecules and three RNA molecules with a combined molecular weight of 2.7 MDa. Even though, in this case, the crystals are relatively large (up to 500 μm in the largest dimension), there is a dramatic variability in their diffraction quality, with diffraction limits varying from 6 Å to 2.8 Å. Venki Ramakrishnan's (MRC-LMB, Cambridge) and Ada Yonath's (Weizmann Institute, Israel Nobel Prize in 2009) groups routinely screened many hundreds of crystals in order to find those best suited for data collection. Often screening was carried out on one beamline where frequent access was possible and then data collected at a beamline that was optimised for the measurement for crystals with large unit cell dimensions (Schlunzen et al, 2001; Selmer et al, 2006).

These examples are typical of many ongoing structural biology projects. Access to highly automated, high throughput screening facilities, with the possibility to then transfer the best crystals to another beamline optimised for data collection, will

become an increasingly important element for success in Structural Biology. In practice, the ability to identify those "one in a thousand" samples that are well ordered will enable new science to be performed with new projects becoming viable. Such a crystal evaluation facility would be unique and, in the provision of this facility, the ESRF would maintain its world-leading role in the development of Structural Biology and as a provider of innovative synchrotron radiation instrumentation.

In essence, UPBL10 will provide an upgraded set of beamlines regenerating ID14 A&B on ID30. The project consists of a suite of beamlines. Three end-stations will provide facilities for different types of sample evaluation: testing the diffraction resolution limit, locating the best part of a crystal on which to perform data collection, detecting the presence of anomalous scatterers, screening for bound inhibitors and ligands, screening in crystallisation plates. **The screening stations directly address a fundamental problem in modern Structural Biology – that of inter and intra sample variability** and will have different beam sizes (two stations with 100 µm beam diameter and one microbeam station with a beam size of 10-20 µm in diameter).

Identifying the “best” crystal is only the beginning of a successful MX experiment. UPBL10 will also provide a tuneable end-station, from an independent canted source, to provide a facility optimised for the data collection requirements of many crystals identified as being suitable. Exploiting the potential of a high β source, this end-station will have a relatively large beam (~200 µm) with an X-ray collimation system able to tailor the size and shape of the beam to that of the sample. This will increase signal-to-noise ratios, thus maximising the number of reflections observed and reducing the exposure times required for the collection of high quality data. The low divergence of the beam will also be extremely useful in data collection from crystals with large unit cells (>1000 Å). The end-station could also be specialised in low resolution studies (d_{min} to ~1000 Å) and be optimised for the measurement of very weak anomalous scattering signals. Additionally, there could be a permanently mounted on-line micro-spectrophotometer.

The bending magnet beamline BM29 will be modified for bioSAXS/Protein Solution Scattering (replacing ID14-3). The totality of our proposal will thus amalgamate the synchrotron radiation facilities required by structural biologists for the next 10 to 15 years. The integrated resources centered around ID23, BM29, ID29 and ID30 will provide a set of beamlines for the collection of the highest quality diffraction data and BIOSAXS data from the wide variety of samples that will arise from Structural Biology studies of challenging biological problems. It will also be able to cope with the projected three- to five-fold increase in sample numbers arising from the search for appropriate crystals from which to collect data.

The close proximity of ID30, ID29 and BM29 enables synergistic effects with respect to sharing space for laboratories, remote access control cabins, the anticipated dewar storage and sample sorting area and storage areas for other ancillary equipment such as micro-spectrophotometers, sample dehydration devices, and others. An additional advantage is that the time between crystal evaluation and data acquisition will be minimised by an improved sample flow between end-stations. This will be beneficial both for the experiment and the operation of the beamlines.

In a field that is as competitive as Structural Biology, an upgraded MX resource that is readily accessible to all European researchers is of paramount importance. The ESRF has been a leader in the provision of the "first generation" of automation for MX beamlines, a development that has been ongoing for almost five years. This level of automation is only now being partially implemented at national synchrotron sources. The expertise acquired at the ESRF during the deployment of our automation developments makes it ideally and uniquely suited to embark on the provision of "second generation" automated MX facilities. These will provide a paradigm shift for MX experiments which will benefit the entire European Structural Biology community. The upgrade of the ESRF's MX resources proposed here will provide unparalleled facilities for Structural Biology leaving the ESRF uniquely placed to support and lead the development of Structural Biology over the next 20 years.

While instrument provision will offer the means to allow UPBL10 to operate, its success will be ensured by the development of suitable software. In this context, the ESRF will build on its proven leadership in the development of automated beamline control (mxCuBE), data management (ISPyB (Beteva et al, 2006)) and sample evaluation (DNA (Leslie et al, 2002) and BEST (Popov & Bourenkov, 2003)). New methods will be developed in order to meet the challenges presented by UPBL10. Based on previous experience we expect that these developments will benefit the broader European MX community; DNA/BEST is in use at all operational light sources in Europe (as well as many in the US and Australia) and ISPyB and mxCuBE are available at six European sites. Thus we expect to continue our history of collaboration with all SR facilities and contribute to the success of MX on a European scale.

1.4 TECHNICAL CONSIDERATIONS

The scientific case defines UPBL10 as a dedicated facility optimised for high throughput automatic sample evaluation and selection and specialised data collection featuring:

- Three fixed wavelength (14 keV) end-stations with high throughput sample evaluation and data collection stations. Two stations with 80 µm beam diameter, one microbeam of 10-20 µm in diameter.
- An independent tuneable (5 – 20 keV) end-station with adjustable beam size (20 µm – 200 µm) and specialisation for very low resolution data collection and detection of very weak anomalous signals.

These considerations lead us to propose the enlargement of the straight section of ID30 to 6 metres, which would enable a canted source providing two independent lines from a single straight section. This layout is essential to the provision of specialised, independent data collection and sample evaluation end-station and fulfils the demands of the European MX User Community. In order to achieve sufficient spatial separation of the beams the experimental hutch of the tuneable end station needs to be placed at around 100 m from the X-ray source.

X-ray source

Source and undulators:
The configuration below (Figure 2) shows a set-up of two canted undulators located on a 6 m ID30 straight section. The canting angle at this stage is taken at +/- 2.2 mrad, if possible.

In order to roughly estimate the photon flux available at the sample position, initial calculations (Table 3) have been made for the photon flux at the position of the primary slits (27 metres) with an aperture of 2 mm x 1 mm (H x V) and with a ring current of 200 mA. For reference, the values calculated as in October 2008 for end stations on ID14 and ID23-1 are 1.3 x 10^{14} ph/s/0.1%bw and 2.2 x 10^{14} ph/s/0.1%bw, respectively.

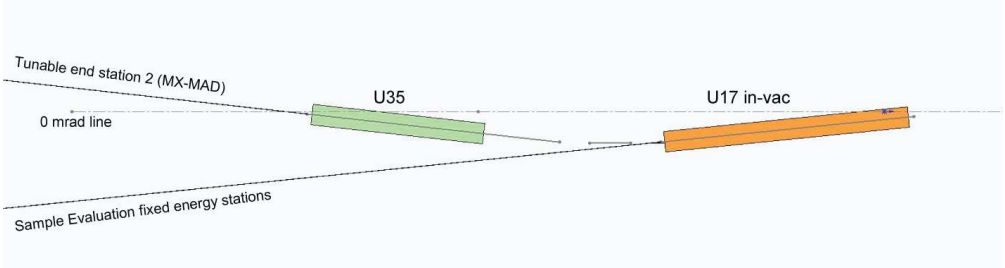

Figure 2. Canted undulator setup for UPBL10 on the ID30 straight section.

	Undulator	Photons flux (14 keV)	Energy range (keV)	Spot size
UPBL10 MASSIF	U17 gap: 6 mm; 14 keV In vacuum	1.8 x 10^{15} ph/s/0.1%bw	14	2 x 100 µm 1 x 10-20 µm
UPBL10 tuneable	U35 gap:15 mm; 14 keV	4 x 10^{14} ph/s/0.1%bw	6 – 20	20 – 200 µm

Table 3: Estimates of flux expected at the sample positions on UPBL10.

Front end:
The front end should be capable of transmitting the photon flux from the canted undulators defined above. It allows an unrestricted opening of the primary slits situated at 27 metres of up to 3 mm x 2 mm (H x V).

General layout and concept for optical design:

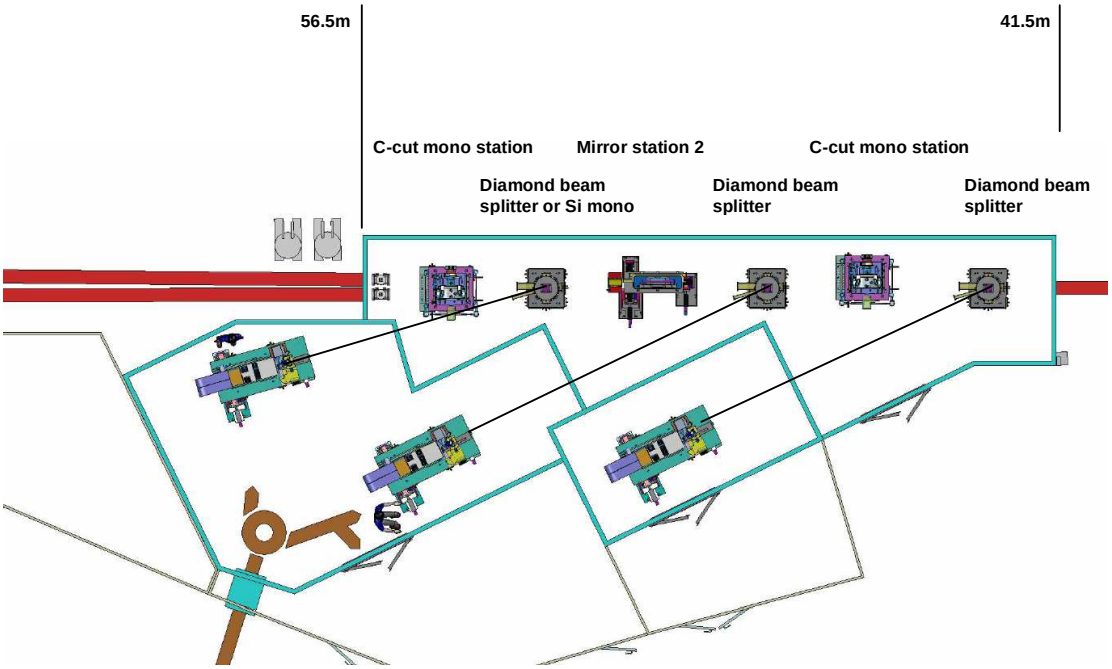

Figure 3. Possible layout of the optical hutch 2 of UPBL10 and the experimental hutches for the sample evaluation facility. A small optics hutch situated upstream will contain primary slits and beam diagnostics. Appropriate focussing elements are currently under discussion with the Optics Group.

This optical layout would give a hutch/control cabin layout as indicated below when integrated into the available space of EX1.

Phasing of project

The full project can be considered as a series of phases which, when finished, achieve the goal of an integrated MX facility.

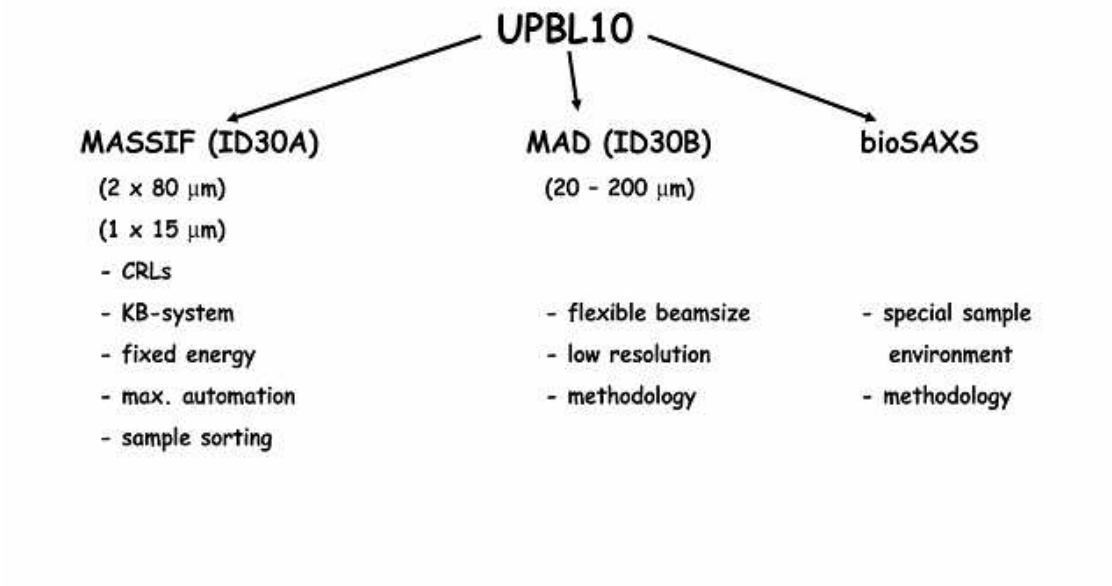

Experimental hutches

The experimental hutch for the tuneable end-station should be comparable with those that already exist as MX experimental hutches. It will be equipped with standard MX equipment such as a set of beam cleaning and beam defining apertures, a set of attenuators, a cryogenic cooling device for keeping the samples at 100 K, a fluorescence detector and an automated sample changer and a single axis diffractometer with a sphere of confusion at least equivalent to the one on the current diffractometer, *i.e.* better than 2 μm. Potentially, the hutch could be equipped with a flat silicon mirror close to the sample position to remove third harmonic reflection contamination at low energies and UV laser for crystal centering. The X-ray image detector, one of the keystones of the experiment itself is discussed in a separate paragraph below.

The end-stations dedicated to evaluation will also be equipped with the devices listed above except the sample changer and diffractometer. In order to speed up the process, one key idea is to have a robot that can be used both as a sample changer and a diffractometer. This challenge is under investigation in collaboration with the FIP CRG beamline team and the EMBL instrumentation group. The general feasibility of such an experiment has already been shown but with an increased sphere of confusion of the rotating axis

Sample Sorting Facility

The core of UPBL10 is the sample sorting facility where samples evaluated on the three evaluation end-stations will be re-distributed to the data collection end-station best suited to perform the experiment (Figure 4). To cope with the expected (high) number of samples and to keep the time between sample evaluation and data collection as short as possible, a high degree of automation is essential.

The possibility of having one end-station with two incoming beams could be envisaged, for example one microbeam (10-20 μm) and one standard beam (80 μm). This would allow use of a shared sample sorting device between the two experiments. The admission and removal of those samples will also be automated.

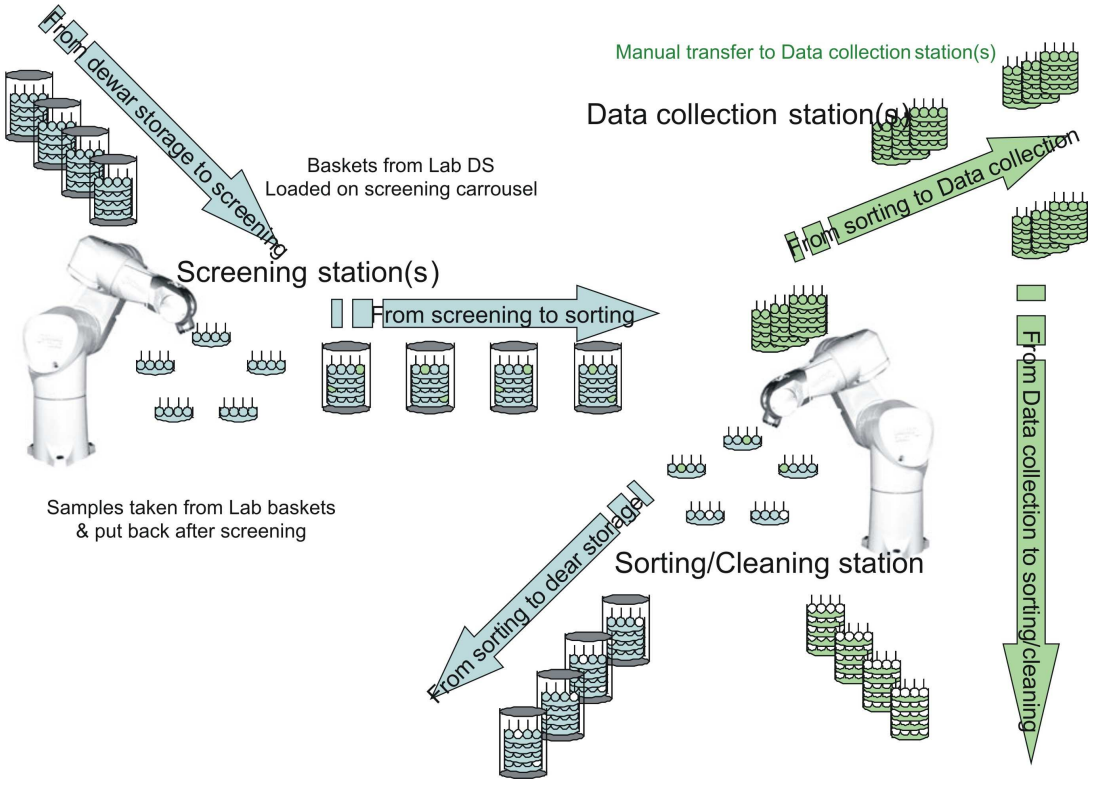

Figure 4. Possible work flow of samples in the sample sorting facility.

Technical challenges

The automation of the screening of thousands of samples a day and their subsequent relocation to the most appropriate beamline for data collection will be one of the challenges this project will have to face and overcome. This success is linked to the development of an automated way of unloading of samples from sent dewars and being able to track them with information management and experiment optimisation.

Table 4 below summarises the characteristics of the end-stations proposed in UPBL10.

	Evaluation side stations				
Energy	**Station 1**	**Station 2**	**Station 3**	**MAD station**	**BioSASX (BM29)**
Flux on sample through 100 x 100 µm aperture	At least 10^{12} ph/s	At least 10^{12} ph/s	At least 10^{12} ph/s	4 x 10^{12} ph/s @14 keV	At least 5 x 10^{12} ph/sec @ 13 keV
Minimum focal spot size µm (FWHM)	80	80	30 - 40	200	700
Spot size range using apertures µm			10 - 20	20 - 200	100 - 700
Energy range	Fixed 14 keV			6 -20 keV	7 – 15 keV
Energy resolution	low 10^{-4}			low 10^{-4} Possibility 311 mono	

Table 4: Summary characteristics of the UPBL10 end-stations.

1.5 REFERENCES

Ben-Shem A, Frolow F, Nelson N (2003) Crystal structure of plant photosystem I. *Nature* **426**(6967)**:** 630-635.

Beteva A, Cipriani F, Cusack S, Delageniere S, Gabadinho J, Gordon EJ, Guijarro M, Hall DR, Larsen S, Launer L, Lavault CB, Leonard GA, Mairs T, McCarthy A, McCarthy J, Meyer J, Mitchell E, Monaco S, Nurizzo D, Pernot P, Pieritz R, Ravelli RG, Rey V, Shepard W, Spruce D, Stuart DI, Svensson O, Theveneau P, Thibault X, Turkenburg J, Walsh M, McSweeney SM (2006) High-throughput sample handling and data collection at synchrotrons: embedding the ESRF into the high-throughput gene-to-structure pipeline. *Acta Crystallogr D Biol Crystallogr* **62**(Pt 10)**:** 1162-1169.

Cipriani F, Felisaz F, Launer L, Aksoy JS, Caserotto H, Cusack S, Dallery M, di-Chiaro F, Guijarro M, Huet J, Larsen S, Lentini M, McCarthy J, McSweeney S, Ravelli R, Renier M, Taffut C, Thompson A, Leonard GA, Walsh MA (2006) Automation of sample mounting for macromolecular crystallography. *Acta Crystallogr D Biol Crystallogr* **62**(Pt 10)**:** 1251-1259.

Cockburn JJ, Abrescia NG, Grimes JM, Sutton GC, Diprose JM, Benevides JM, Thomas GJ, Jr., Bamford JK, Bamford DH, Stuart DI (2004) Membrane structure and interactions with protein and DNA in bacteriophage PRD1. *Nature* **432**(7013)**:** 122-125.

Coureux PD, Wells AL, Menetrey J, Yengo CM, Morris CA, Sweeney HL, Houdusse A (2003) A structural state of the myosin V motor without bound nucleotide. *Nature* **425**(6956)**:** 419-423.

Cramer P, Bushnell DA, Kornberg RD (2001) Structural basis of transcription: RNA polymerase II at 2.8 angstrom resolution. *Science* **292**(5523)**:** 1863-1876.

Dawson RJ, Locher KP (2006) Structure of a bacterial multidrug ABC transporter. *Nature* **443**(7108)**:** 180-185.

Doyle DA, Morais Cabral J, Pfuetzner RA, Kuo A, Gulbis JM, Cohen SL, Chait BT, MacKinnon R (1998) The structure of the potassium channel: molecular basis of K^+ conduction and selectivity. *Science* **280**(5360)**:** 69-77.

Ferreira KN, Iverson TM, Maghlaoui K, Barber J, Iwata S (2004) Architecture of the photosynthetic oxygen-evolving center. *Science* **303**(5665)**:** 1831-1838.

Flot D, Mairs T, Giraud T, Guijarro M, Lesourd M, Rey V, van Brussel D, Morawe C, Boral C, Hignette O, Chavanne C, Nurizzo D, McSweeney S, Mitchell E (2008) The ID23-2 Structural Biology Microfocus Beamline at the ESRF. Submitted J. Synch. Rad.

Grimes JM, Burroughs JN, Gouet P, Diprose JM, Malby R, Zientara S, Mertens PP, Stuart DI (1998) The atomic structure of the bluetongue virus core. *Nature* **395**(6701)**:** 470-478.

Groll M, Ditzel L, Lowe J, Stock D, Bochtler M, Bartunik HD, Huber R (1997) Structure of 20S proteasome from yeast at 2.4 A resolution. *Nature* **386**(6624)**:** 463-471.

Jacquamet L, Ohana J, Joly J, Borel F, Pirocchi M, Charrault P, Bertoni A, Israel-Gouy P, Carpentier P, Kozielski F, Blot D, Ferrer JL (2004a) Automated analysis of vapor diffusion crystallization drops with an X-ray beam. *Structure* **12**(7)**:** 1219-1225.

Jacquamet L, Ohana J, Joly J, Legrand P, Kahn R, Borel F, Pirocchi M, Charrault P, Carpentier P, Ferrer JL (2004b) A new highly integrated sample environment for protein crystallography. *Acta Crystallogr D Biol Crystallogr* **60**(Pt 5)**:** 888-894.

Janssen BJ, Huizinga EG, Raaijmakers HC, Roos A, Daha MR, Nilsson-Ekdahl K, Nilsson B, Gros P (2005) Structures of complement component C3 provide insights into the function and evolution of immunity. *Nature* **437**(7058)**:** 505-511.

Leslie AG, Powell HR, Winter G, Svensson O, Spruce D, McSweeney S, Love D, Kinder S, Duke E, Nave C (2002) Automation of the collection and processing of X-ray diffraction data -- a generic approach. *Acta Crystallogr D Biol Crystallogr* **58**(Pt 11)**:** 1924-1928.

Liu Y, Hong X, Kappler J, Jiang L, Zhang R, Xu L, Pan CH, Martin WE, Murphy RC, Shu HB, Dai S, Zhang G (2003) Ligand-receptor binding revealed by the TNF family member TALL-1. *Nature* **423**(6935)**:** 49-56.

Ohana J, Jacquamet L, Joly J, Bertoni A, Taunier P, Michel L, Charrault P, Pirocchi M, Carpentier P, Borel F, Kahn R, Ferrer JL (2004) CATS: a cryogenic automated transfer system installed on the beamline FIP at ESRF. *Journal of Applied Crystallography* **37:** 72-77.

Ormo M, Cubitt AB, Kallio K, Gross LA, Tsien RY, Remington SJ (1996) Crystal structure of the Aequorea victoria green fluorescent protein. *Science* **273**(5280)**:** 1392-1395.

Popov AN, Bourenkov GP (2003) Choice of data-collection parameters based on statistic modelling. *Acta Crystallogr D Biol Crystallogr* **59**(Pt 7)**:** 1145-1153.

Schlunzen F, Zarivach R, Harms J, Bashan A, Tocilj A, Albrecht R, Yonath A, Franceschi F (2001) Structural basis for the interaction of antibiotics with the peptidyl transferase centre in eubacteria. *Nature* **413**(6858)**:** 814-821.

Selmer M, Dunham CM, Murphy FVt, Weixlbaumer A, Petry S, Kelley AC, Weir JR, Ramakrishnan V (2006) Structure of the 70S ribosome complexed with mRNA and tRNA. *Science* **313**(5795)**:** 1935-1942.

Sung BJ, Hwang KY, Jeon YH, Lee JI, Heo YS, Kim JH, Moon J, Yoon JM, Hyun YL, Kim E, Eum SJ, Park SY, Lee JO, Lee TG, Ro S, Cho JM (2003) Structure of the catalytic domain of human phosphodiesterase 5 with bound drug molecules. *Nature* **425**(6953)**:** 98-102.

Walker JE (1998) ATP synthesis by rotary catalysis (Nobel lecture). *Angewandte Chemie - international edition* **37:** 2309-2319.

Warne T, Serrano-Vega MJ, Baker JG, Moukhametzianov R, Edwards PC, Henderson R, Leslie AG, Tate CG, Schertler GF (2008) Structure of a β_1-adrenergic G-protein-coupled receptor. *Nature* **454**(7203)**:** 486-491.

Williams PA, Cosme J, Vinkovic DM, Ward A, Angove HC, Day PJ, Vonrhein C, Tickle IJ, Jhoti H (2004) Crystal structures of human cytochrome P450 3A4 bound to metyrapone and progesterone. *Science* **305**(5684)**:** 683-686.

Williams PA, Cosme J, Ward A, Angove HC, Matak Vinkovic D, Jhoti H (2003) Crystal structure of human cytochrome P450 2C9 with bound warfarin. *Nature* **424**(6947)**:** 464-468.

Zouni A, Witt HT, Kern J, Fromme P, Krauss N, Saenger W, Orth P (2001) Crystal structure of photosystem II from Synechococcus elongatus at 3.8 A resolution. *Nature* **409**(6821)**:** 739-743.